Enhancement of surface NMR by laser-polarized noble gases

T. Rõõm,* S. Appelt,† and R. Seydoux
Materials Sciences Division, Lawrence Berkeley National Laboratory and the Department of Chemistry, University of California, Berkeley, California 94720

E. L. Hahn
Materials Sciences Division, Lawrence Berkeley National Laboratory and the Department of Chemistry, University of California, Berkeley, California 94720 and Department of Physics, University of California, Berkeley, California 94720

A. Pines
Materials Sciences Division, Lawrence Berkeley National Laboratory and the Department of Chemistry, University of California, Berkeley, California 94720

(Received 18 November 1996)

The transfer of spin polarization from laser-polarized helium and xenon to spins such as ^{1}H and ^{13}C on the surface of high-surface-area solids (Aerosil) is demonstrated over a temperature range from 4 to 200 K. The transfer mechanism is dipole-dipole cross relaxation between the spins of the adsorbed mobile noble gas and the surface spins (spin-polarization-induced nuclear Overhauser effect). The enhancement of surface proton magnetization by laser-polarized helium at 4 K and 10 K is between one and twofold. Using laser-polarized xenon, enhancement factors of up to 20 were obtained when compared to the Boltzmann polarization in a field of 4.2 T and at a temperature of 130 K. [S0163-1829(97)02917-2]

I. INTRODUCTION

The ^{129}Xe chemical shift has been widely used to probe the structure of microporous solids, in particular zeolites and clathrates.[1] The NMR parameters of Xe on silica surfaces similar to those used in this study have been studied at 77 K by Cho *et al.*[2] The enhanced NMR sensitivity of ^{129}Xe due to laser polarization has had an impact in a number of areas, among them clinical imaging, [3–5] atomic physics,[6,7] and materials and surface science.[8–15] The transfer of polarization was recently demonstrated between laser-polarized ^{129}Xe in solution and the spins of the solvent, liquid benzene.[16] The mechanism underlying this transfer is the nuclear Overhauser effect[17,18] arising from cross relaxation between spin-polarized xenon and the solution proton spins, an effect termed SPINOE (spin-polarization-induced nuclear Overhauser effect).

In this paper we describe experiments on the transfer of spin polarization from laser-polarized noble gases to nuclear spins on solid surfaces. Some steps in the direction of surface-enhanced NMR have been published,[9,10,13] wherein the signal from surface ^{1}H spins is increased by cross polarization from laser-polarized ^{129}Xe frozen on the surface. This approach requires immobilization of the Xe and a low-field mixing or Hartmann-Hahn frequency matching in the rotating frame, a technique used for signal enhancement of ^{13}C NMR in solids.[19] We show in the present work that the magnetization of ^{1}H and ^{13}C nuclei in differently modified surfaces of high-surface-area solids (Aerosil) can be enhanced in high field (4.2 T). This is achieved by exposing the surfaces to spin-polarized ^{129}Xe or ^{3}He gas. In contrast to previous cross-polarization experiments, the magnetization transfer is established by dipole-dipole cross relaxation of surface spins and mobile gas atoms adsorbed on the surface, a relaxation mechanism analogous to that previously invoked for liquid ^{3}He and surface spins at very low temperatures.[20,21] For one specific surface modification of Aerosil we studied the enhancement of ^{1}H magnetization as a function of temperature and Xe pressure and have measured the temperature dependence of ^{129}Xe chemical shifts and longitudinal relaxation rates of ^{129}Xe and ^{3}He.

II. EXPERIMENTAL SETUP

The main component of the experimental setup (Fig. 1) is a dynamic flow cryostat (Oxford Instruments) which is inserted in the superconducting magnet (4.2 T). NMR data were acquired with a transmission line probe, operating at 180 and 45 MHz, the Larmor frequencies of ^{1}H and ^{13}C at this field. The sample is located at the bottom of an L-shaped glass tube of 1 m in length and with an inner diameter of 6 mm, serving as a transfer line for the laser-polarized gas. Aerosil,[22] composed of silica particles with a mean diameter of 16 nm and a surface area of 130 m^2/g, served as the sample. The Aerosil particles are used either uncoated, coated with physisorbed CO_2, or coated with PEO (polyethylene oxide, molecular mass $\approx$ 400 000, 86 mg per 1 g of Aerosil).

The PEO sample is evacuated at room temperature to 10^{-5} torr for several hours. For the experiments with the uncoated Aerosil, the sample is heated 2 h at 280°C at 10^{-5} torr in order to remove physisorbed water.

The optical pumping (OP) cell has a volume of 10 cm^3 and is filled with a small amount of Rb metal, either 80% enriched ^{129}Xe (1 atm at room temperature) or 99.9% enriched ^{3}He (2 atm at room temperature) and about 100–200

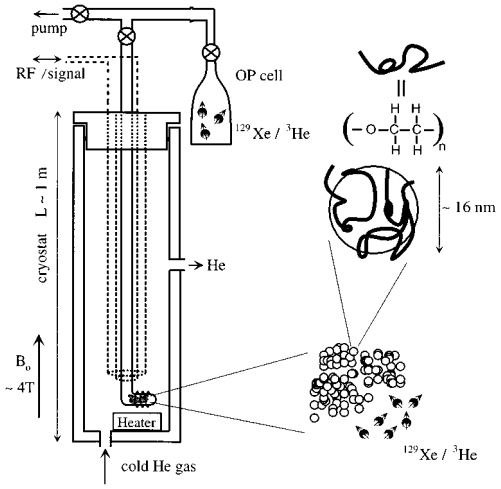

FIG. 1. Experimental setup for the study of SPINOE on surfaces with spin-polarized noble gases. The optical pumping (OP) cell, containing the laser-polarized gas, is connected to a Pyrex glass tube, leading down to the sample region. The sample consists of Aerosil particles coated or uncoated with polyethylene oxide (the coated particles are shown schematically in the figure). The whole cryostat is fitted into an NMR magnet (not shown), providing a field of 4.2 T at the sample. The dotted lines denote the coaxial tubes for the radio frequency transmission.

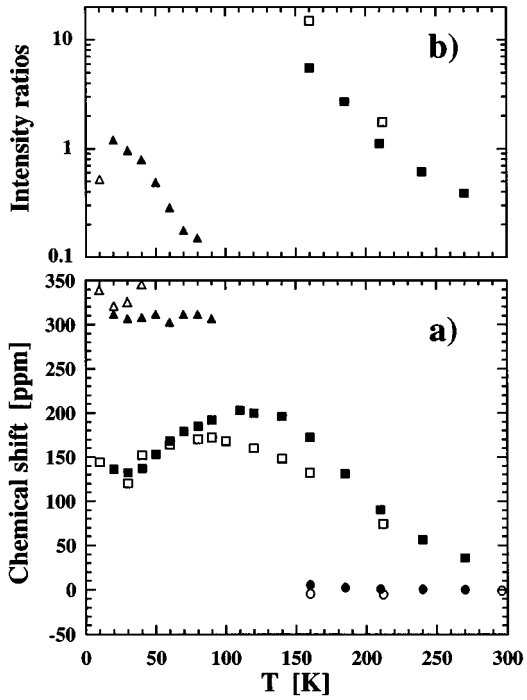

FIG. 2. Temperature dependence of NMR line positions and intensity ratios of ^{129}Xe signals in sealed PEO samples. The open and solid symbols correspond to Xe pressures of 2.5 atm and 10 atm, respectively. (a) ^{129}Xe chemical shift in the PEO sample as a function of temperature: (○) gas, (□) adsorbed, and (△) solid Xe phases. (b) Ratio of intensities, taken as integrals from the ^{129}Xe spectrum, between adsorbed to gas phase (□) and solid to adsorbed phase (△) as a function of temperature.

torr of N_2 in order to quench the Rb fluorescence. The cell is placed in a 40 G magnetic field of Helmholtz coils and heated to 95 °C (Xe pumping) or 190 °C (He pumping). The Rb atoms are optically pumped at the wavelength (794.8 nm) of the Rb D_1 transition with 1 W circularly polarized light from a Ti-sapphire laser for 20 min (Xe) or for 60 min (He). The noble gas nuclei reach spin polarizations of about 10%.

After cooling to room temperature, the optical pumping cell is then attached to the NMR probe. Upon brief evacuation of the connecting glassware, the OP cell is then opened to the precooled sample space.

The time evolution of the surface magnetization is monitored by applying small tipping angle pulses (10°–20°) and recording the free induction decay.

Spin lattice relaxation rates and chemical shifts of ^{3}He and ^{129}Xe atoms on the PEO surface were obtained from three sealed glass samples (1.5 cm^3 in volume), each containing 250 mg of PEO powder and filled with 2.5 atm of ^{3}He gas or 2.5 and 10 atm of ^{129}Xe gas.

III. RESULTS AND DISCUSSION

A. ^{129}Xe chemical shift

Figure 2(a) shows the peak positions of the ^{129}Xe NMR spectra for the PEO sample as a function of temperature. Three regimes of chemical shifts can be discerned, corresponding to Xe in the gas, adsorbed, and solid phases. The chemical shifts of Xe in the gas and solid phases change little with temperature, whereas the chemical shift of the adsorbed phase increases from 35 ppm at $T=270$ K (for the 10 atm sample) to a maximum value of 200 ppm at $T=110$ K and finally decreases to 130 ppm at $T=30$ K.

Two possible mechanisms suggest themselves for this behavior. First, at high temperatures, the rapid exchange between Xe atoms in the void spaces and adsorbed on the surface of the PEO powder leads to an average value for the measured chemical shift. The separate gas peak is present because only the lower half part of the sample volume is filled with powder and the gas atoms in the upper region do not exchange rapidly with the PEO surface. As the temperature decreases, the ratio between adsorbed and gas Xe signals rises exponentially, as indicated in Fig. 2(b), leading to an increase in the average value of the chemical shift. The second mechanism, also expected to lead to an increase of the chemical shift at lower temperatures, arises from Xe-Xe interactions in the adsorbed layer which grow as the temperature decreases. At $T=110$ K, all the gas is adsorbed on the 30 m^2 surface area of PEO, giving an estimated Xe film thickness of about one monolayer for the 10 atm sample.

The decrease of the chemical shift below 110 K can be explained by the onset of xenon freezing, as indicated by the increase of the ratio of signals from the solid and adsorbed phases [Fig. 2(b)].[23] The crystallization of Xe atoms into solid regions decreases the number of adsorbed xenon atoms, thus reducing the contribution of Xe-Xe interactions to the chemical shift of the adsorbed film. The observed maximum chemical shift of 160 ppm for the adsorbed Xe in the 2.5 atm sample (open squares) is 40 ppm lower than the corresponding shift for the 10 atm sample, supporting the model of contributions from Xe-Xe interactions to the chemical shift of Xe in the adsorbed state.

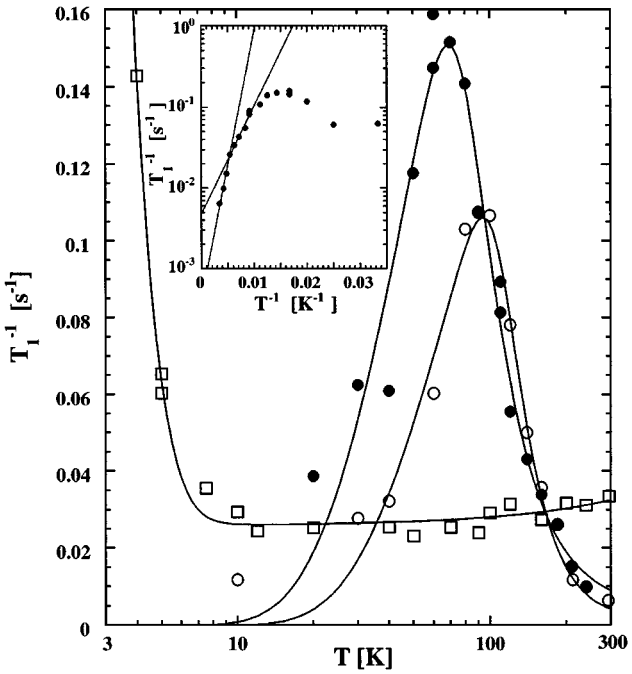

FIG. 3. Temperature dependence of ^{3}He and adsorbed ^{129}Xe T_1 relaxation rates in sealed PEO samples. (□) 2.5 atm of ^{3}He, (○) 2.5 atm of Xe, (●) 10 atm of Xe. Solid lines are drawn to guide the eye. The inset shows fits $y=a\exp(-E_{Ai}/kT)$ with $a=4.1\times10^{-4}$ s^{-1}, $E_{A1}=-70$ meV for the high-temperature and $a=4.7\times10^{-3}$ s^{-1}, $E_{A2}=-30$ meV for the lower-temperature rising regions of the relaxation curve of the 10 atm Xe sample. A similar type of fit for ^{3}He gives $E_A=-1.4$ meV.

Below 30 K the shifts of the adsorbed peak do not change considerably with temperature and seem to be independent of the amount of Xe, indicating that this shift is dominated by interactions with the surface.

B. ^{3}He and ^{129}Xe relaxation

Figure 3 shows the measured T_1 relaxation rates of ^{3}He and adsorbed ^{129}Xe on the PEO surface as a function of temperature. While the Xe relaxation rates exhibit maxima at 70 K and 110 K, the ^{3}He relaxation rate does not change substantially from room temperature down to $T=10$ K, but increases rapidly below 10 K.

For both ^{3}He and ^{129}Xe the rising relaxation rates in the high-temperature regime of the relaxation curves can be explained by a thermally activated motion of the noble gas atoms, leading to a modulation of the dipole-dipole coupling between the gas atoms and the ^{1}H spins of the PEO surface. The relaxation rate ρ_S of the S spins, due to the modulation of the dipole-dipole interaction between I (^{1}H or ^{13}C) and S spins (^{3}He or ^{129}Xe), is given by[24]

$$\rho_S=\frac{1}{10}\rho_{0S}\left(\frac{1}{1+(\omega_{0I}-\omega_{0S})^2\tau_c^2}+\frac{3}{1+\omega_{0S}^2\tau_c^2}+\frac{6}{1+(\omega_{0I}+\omega_{0S})^2\tau_c^2}\right), \quad (1)$$

where ω_{0I} and ω_{0S} are the Larmor frequencies of the I and S spins and ρ_{0S} is the relaxation rate in the fast motion limit $[(\omega_{0I}\pm\omega_{0S})^2\tau_c^2\ll1]$. The relaxation rate ρ_{0S} can be expressed as

$$\rho_{0S}=\tfrac{4}{3}I(I+1)\gamma_I^2\gamma_S^2\hbar^2\tau_c\sum_i r_i^{-6}, \quad (2)$$

where r_i is the distance between S and I_i spins, γ_S, γ_I are the corresponding magnetogyric ratios of the spins, and the sum is taken over the I spins. The correlation time τ_c at the binding sites is related to the activation energy E_A and hopping rate τ_0^{-1} as

$$\tau_c=\tau_0\exp(-E_A/kT). \quad (3)$$

The analytical function, Eq. (1), does not fit the measured Xe relaxation rates over the entire temperature range. Equation (1), as a function of $1/T$, has a characteristic maximum at the temperature at which $\omega_{0S}\tau_c\approx1$. It can be seen (Fig. 3) that the maximum in the Xe relaxation rate depends on the amount of xenon on the PEO surface, while Eq. (1) is independent of the number of gas atoms on the surface. This behavior is attributed to Xe-Xe interactions, changing the mobility of xenon on the surface. The deviations from Eq. (1) on the low-temperature side of the maxima (long correlation times) are possibly caused by paramagnetic impurities and the freezing of Xe.

Thus, the activation energies E_A for the motion of He and Xe atoms on the PEO surface are determined for our data in the short-correlation-time limit $[(\omega\tau_c)^2\ll1]$ of Eq. (1), where $\rho_S=\rho_{0S}$. For the ^{129}Xe relaxation, two different regions can be observed in the temperature dependence on the high-temperature side of the $1/T_1$ data with a crossover temperature at 200 K, yielding two apparent activation energies $E_{A1}=-70$ meV (-810 K) above 200 K and $E_{A2}=-30$ meV (-350 K) below 200 K. The first energy value is similar to the Xe binding energy previously measured for a glass surface coated with Surfasil (-100 meV).[14] The second energy value is most probably related to the motion of the Xe on the PEO surface, with $E_{A2}=-30$ meV being the mean value of the energy barrier height between trapping sites. For $T>200$ K the ^{129}Xe spin interactions with the surface spins are modulated by the exchange of Xe atoms between surface adsorbed states and the gas phase. For $T<200$ K the residence time of the Xe atoms on the surface becomes long and the modulation mechanism for the spin interactions is the thermally activated hopping on the surface between different trapping sites. For ^{3}He the investigated temperature is not low enough to observe the maximum in the relaxation curve (Fig. 3). A fit at 10 K$>T>$4 K results in $E_A=-1.4$ meV (-16 K).

C. SPINOE

Figures 4–7 show the evolution of the magnetization of surface ^{1}H and ^{13}C spins after exposure of the surface to the laser-polarized ^{129}Xe or ^{3}He gas. Each point in the plots represents the integral of the Fourier-transformed free induction decay, proportional to the instantaneous total nuclear magnetization. The insets show the corresponding ^{1}H or ^{13}C spectra at the Boltzmann equilibrium (positive peak) and

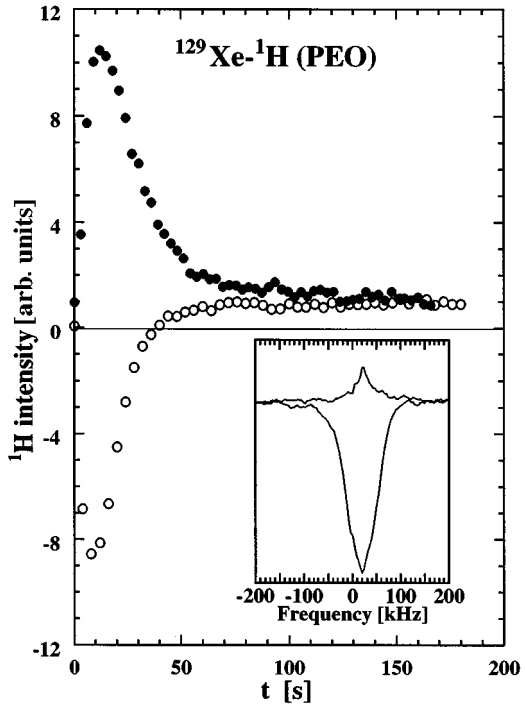

FIG. 4. Evolution of the ^{1}H spin magnetization of PEO-coated Aerosil130 as a function of time after exposure of the surface to laser-polarized ^{129}Xe. The initial Xe pressure, prior to adsorption, is 160 torr and the sample temperature is 130 K for the positive SPINOE (●) and 125 K for the negative SPINOE (○). The inset displays two single-shot ^{1}H spectra from the negative SPINOE run, one taken at Boltzmann equilibrium for the unpolarized sample (positive peak) and the other taken at the time t_0, when the negative SPINOE enhancement has reached its maximum absolute value.

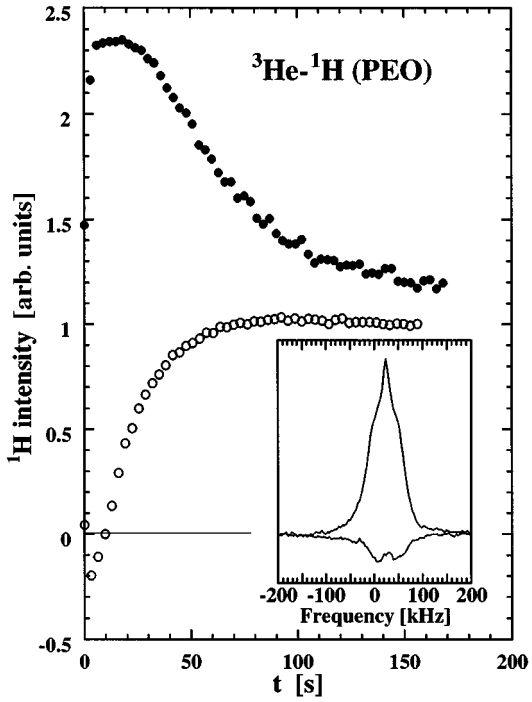

FIG. 5. Evolution of the ^{1}H spin magnetization of PEO coated Aerosil130 as a function of time after exposure of the surface to laser-polarized ^{3}He. The initial He pressure (in a volume of 40 cm^3), prior to adsorption, is 360 torr and the sample temperature is 10 K for the positive SPINOE (●) and 4 K for the negative SPINOE (○). The inset displays two single-shot ^{1}H spectra from the negative SPINOE run, one taken at Boltzmann equilibrium for the unpolarized sample (positive peak) and the other taken at the time t_0, when the negative SPINOE enhancement has reached its maximum absolute value.

after the polarized noble gas has resulted in an enhancement of the surface magnetization. The enhanced spectra are all shown for the times t_0 when the negative enhancement has reached a maximum.

Figure 4 demonstrates the time evolution of the enhanced proton magnetization of PEO with two opposite initial ^{129}Xe magnetizations.[25] The maximum ^{1}H magnetization at $T=130$ K is established after 15 s and is found to be 10 times the Boltzmann magnetization of the total number of proton spins. The decay of the ^{1}H magnetization, after the maximum (minimum) has been reached, is exponential and, according to the Solomon equations,[26] is determined by the Xe T_1 relaxation time. Decay times of ^{1}H magnetization are 20 s at $T=130$ K and 12 s at $T=120$ K, in accordance with the Xe relaxation data on the PEO (Fig. 3). The time evolution of the increasing part of the ^{1}H magnetization is determined not only by the proton T_1 (9 s in our case), but also by the dynamics of the adsorption process of the Xe gas on the surface, including the thermalization of the room temperature gas on the substantially colder surface. The insets (Figs. 4 and 5) show that in PEO the enhancement of ^{1}H magnetization is not uniform in the spectral domain, indicating different enhancements for different ^{1}H species on the surface as well as a small unenhanced ^{1}H background.

In order to investigate the SPINOE of ^{3}He on the PEO surface we measured the ^{3}He adsorption as a function of temperature and found that the He gas begins to adsorb only below 20 K and consequently an efficient SPINOE experiment can only be conducted in this temperature regime. The plot in Fig. 5 shows the enhancement of surface ^{1}H magnetization with laser-polarized ^{3}He. The fractional enhancement [Eq. (4)] at the extrema is 1.4 at 10 K and -1.2 at 4 K. Note that the rate constants of the buildup and decay of the proton magnetization at 4 K are approximately 2 times greater than at 10 K, indicating the stronger ^{3}He interactions with the surface at 4 K.

Figures 6 and 7 give examples of SPINOE from ^{129}Xe on surfaces other than PEO coated Aerosil. Figure 6 shows the enhancement of the ^{1}H magnetization on Aerosil130. Most of the ^{1}H on the surface is found[22] in bound hydroxyl (OH) groups with an average ^{1}H density of 2.5 OH groups per nm^2. Thus, the ^{1}H spins on the glass occur in a single layer and are well isolated from each other, leading to a relatively narrow proton line compared to that of the PEO sample (insets in Figs. 4 and 5). The total number of ^{1}H spins on the Aerosil surface is calculated to be 2×10^{19}, approximately 50 times less than the corresponding number in the PEO sample. Under these conditions a maximum enhancement of 20 is found for the ^{1}H magnetization.

Figure 7 demonstrates the possibility of SPINOE effects to nuclei other than protons, such as ^{13}C. The sample tube containing the Aerosil300 (300 m^2/g surface area) was filled with 99% ^{13}C enriched CO_2 gas. After slowly cooling down

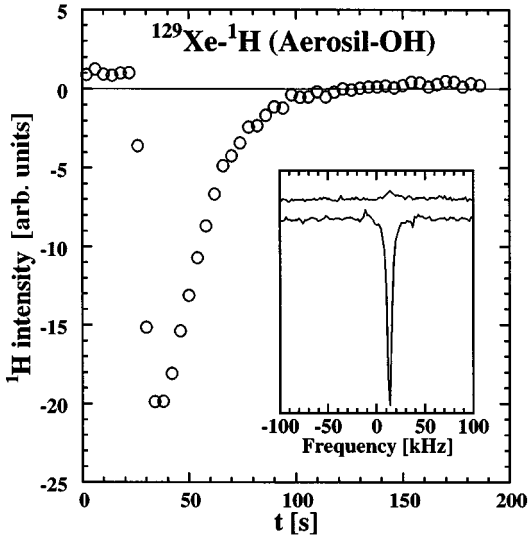

FIG. 6. Negative enhancement of the ^{1}H spin magnetization of surface OH-groups on Aerosil130 after exposure of the surface to laser-polarized ^{129}Xe. The initial Xe pressure is 160 torr and the sample temperature is 130 K. This time, the measurement includes several acquisitions prior to the adsorption. The inset displays two single-shot ^{1}H spectra, one taken at Boltzmann equilibrium for the unpolarized sample (positive peak) and the other taken at the time t_0, when the negative SPINOE enhancement has reached its maximum absolute value.

to $T=130$ K, all the CO_2 molecules are adsorbed on the 20 m^2 surface of the Aerosil powder. The amount of the gas (5×10^{20} molecules) is selected so as to form approximately one to two monolayers of CO_2 on the Aerosil surface. In Fig. 7 the negative SPINOE of ^{13}C reaches a fractional enhancement of -4. The spectra in the inset show that the ^{13}C linewidth of the adsorbed CO_2 molecules is 1.5 KHz (i.e., 34 ppm), which is much narrower than expected from immobile adsorbed CO_2.[27] This observation, together with the relatively short T_1 relaxation time of 1.5 s at 130 K, indicates that the CO_2 molecules are rapidly reorienting on the surface.

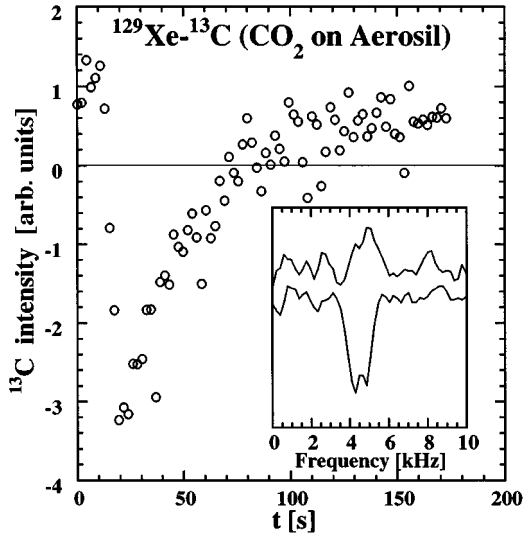

FIG. 7. Negative enhancement of the ^{13}C spin magnetization of CO_2 on Aerosil300 after exposure of the surface to laser-polarized ^{129}Xe. The initial Xe pressure is 160 torr and the sample temperature is 130 K. The ^{13}C-enriched CO_2 covers the Aerosil with one to two monolayers. The inset displays two single-shot ^{13}C spectra, one taken at Boltzmann equilibrium for the unpolarized sample (positive peak) and the other taken at the time t_0, when the negative SPINOE enhancement has reached its maximum absolute value.

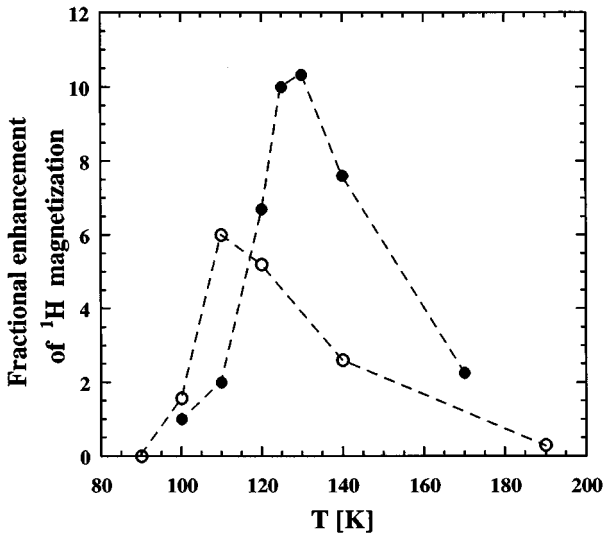

FIG. 8. Absolute value of the fractional enhancement $[I_z(t_0)-I_0]/I_0$ of PEO proton magnetization as a function of temperature and for two different initial Xe pressures: (○) 20 torr, (●) 160 torr. The dotted lines are drawn to guide the eye.

A closer look at Figs. 6 and 7 reveals that the magnetization does not quite recover to the initial value. This is not due to saturation, because for positive SPINOE the signal is observed to remain slightly higher in the end than the equilibrium signal at the beginning. The effect may be attributed to an ongoing exchange at the surface with polarized gas from the large volume of the transfer tube.

D. Temperature dependence of ^{1}H SPINOE

In order to optimize the enhancement of ^{1}H surface magnetization of the PEO sample, we investigated the fractional enhancement $[I_z(t_0)-I_0]/I_0$ [Eq. (4)] of the ^{1}H magnetization as a function of temperature and as a function of Xe pressure.

The initial Xe pressure in the NMR tube was varied by expanding the polarized Xe gas from the pumping cell directly into the sample tube or by expanding it first into an evacuated glass bulb of defined volume. The results are shown in Fig. 8. The solid circles depict the measured fractional ^{1}H enhancements for an initial Xe pressure of 160 torr in a volume of 40 cm^3 (optical pumping cell plus sample tube) and the open circles depict the measured fractional enhancement values for 20 torr of Xe pressure in a total volume of 320 cm^3. Although the total number of Xe atoms (2×10^{20}) is the same for both pressures, there are differences in the temperature dependence of the fractional enhancement. First, the maxima are shifted, and second, the fractional SPINOE is larger at higher pressure: a factor of 10 at $T=130$ K for $p=160$ torr Xe pressure compared to a factor of 6 at $T=110$ K for $p=20$ torr.

One explanation for the temperature shift of the maxima in Fig. 5 is the freezing of Xe onto the glass walls of the sample tube and the formation of solid Xe on the PEO. According to the p-T phase diagram of xenon, at 160 torr the Xe solidification takes place at or below 150 K. This consideration is only valid in the absence of an adsorption process on a high surface area. As indicated by the chemical shift data for the sealed samples (Fig. 2), Xe solidification on the PEO surface is observed above $T=50$ K at 2.5 atm pressure. However, in the sealed samples the pressure drops during the slow cool down due to the adsorption on the high surface area and, in addition, gas atoms are distributed evenly over the surface as they have enough time to penetrate into microscopic pores of the powder. The situation encountered in the SPINOE experiment is intermediate between the sealed sample result and what is expected from the phase diagram. The starting pressure is initially reduced in the SPINOE experiment by the adsorption to the high-surface-area powder but the gas does not have enough time to reach all the pores of the powder on the time scale of the SPINOE (10 s) and begins to freeze onto the glass walls of the sample tube and forms solid Xe on the PEO powder, as experimentally observed by a solid peak in the NMR spectrum of ^{129}Xe at lower temperatures. Nevertheless, the initial pressure is important: At higher initial pressure (160 torr) more gas is delivered to the powder, thus giving a larger SPINOE. At the same time Xe starts to freeze at higher temperatures, thus shifting the maximum of the SPINOE curve to higher temperature compared to the experiments performed at 20 torr of initial pressure.

E. Cross-relaxation rates of SPINOE

In order to estimate the cross-relaxation rate σ_{IS} between gas and surface spins, we use the Solomon equations[26,28] and derive an expression for the maximum change in polarization normalized to the Boltzmann equilibrium magnetization of the surface I spins:

$$\frac{I_z(t_0)-I_0}{I_0}=-\frac{\sigma_{IS}}{\rho_I}\frac{\gamma_S S(S+1)}{\gamma_I I(I+1)}\frac{S_z(t_0)-S_0}{S_0}, \tag{4}$$

where t_0 is the time at which the magnetization of the surface I spins (^{1}H or ^{13}C) has reached a maximum. σ_{IS} is defined as the cross relaxation rate, ρ_I is the autorelaxation rate for the I spins, and I_0 and S_0 are the Boltzmann z components of the I and S spins. $I_z(t_0)$ and $S_z(t_0)$ are the polarizations at the time t_0. The relaxation rate of the I spins can be written as $\rho_I=T_{1I}^{-1}+\rho_I^S$, where T_{1I}^{-1} is the autorelaxation rate of the ^{1}H (^{13}C) spins in the absence of coupling to the noble gas spins and ρ_I^S is the relaxation rate induced by coupling to noble gas spins. In the fast motion limit the cross-relaxation rate σ_{IS} can be related to the relaxation rate of noble gas spins, due to interaction with surface nuclei, ρ_S^I:

$$\sigma_{IS}=\frac{N_S}{2N_I}\rho_S^I. \tag{5}$$

Knowledge of the values $[S_z(t_0)-S_0]/S_0$ and $[I_z(t_0)-I_0]/I_0$ as well as the relaxation rate ρ_I allows a determination of the cross-relaxation rate σ_{IS}. We have measured the quantities $[S_z(t_0)-S_0]/S_0=6000$ for ^{129}Xe (130 K) and $[S_z(t_0)-S_0]/S_0=30$ for ^{3}He (4 K) as well as the ρ_I values for PEO ^{1}H spins ($\rho_I=0.02$ s^{-1} at 4 K, $\rho_I=0.11$ s^{-1} at 130 K) and $\rho_I=0.7$ s^{-1} for ^{13}C spins. The results for the cross-relaxation rates are $\sigma_{IS}=1\times10^{-3}$ s^{-1} for ^{3}He-^{1}H, $\sigma_{IS}=7\times10^{-4}$ s^{-1} for ^{129}Xe-^{1}H, and $\sigma_{IS}=4\times10^{-4}$ s^{-1} for ^{129}Xe-^{13}C.

In the SPINOE experiment on the PEO sample we estimate $N_{\mathrm{Xe}}/N_{\mathrm{H}}=2\times10^{20}/10^{21}=0.2$. If we assume that the main relaxation channel for the Xe spins on the surface is the dipolar interaction with the proton spins ($\rho_S\approx0.06$ s^{-1} at 130 K, Fig. 3), from Eq. (5) we get $\sigma_{IS}=6\times10^{-3}$ s^{-1}. This value is still one order of magnitude higher than deduced from the fractional SPINOE enhancement. One reason for the reduced cross-relaxation rate may be the presence of other relaxation channels for the noble gas spins on the surface, such as paramagnetic impurities and chemical shift anisotropy (for ^{129}Xe). Second, not all the proton spins may be accessible to the gas spins. It is likely that Xe (or He) atoms do not fill all the microscopic pores of the sample on the time scale of the SPINOE and giving a proton ''background'' signal which is not enhanced (as can be seen from the insets of Figs. 4 and 5). Therefore the actual σ_{IS} is larger than determined from the fractional SPINOE enhancement.

IV. CONCLUSIONS

We have demonstrated that laser-polarized ^{3}He and ^{129}Xe, adsorbed on high-surface-area silica, can be used to transfer spin polarization to surface spins, such as ^{1}H and ^{13}C. The transfer mechanism, SPINOE, relies on the cross relaxation between laser-polarized noble gas nuclear spins and surface spins. The magnitude of the SPINOE depends on the cross-relaxation rate and on the number of noble gas spins on the surface. We have shown that with ^{3}He, SPINOE is manifested below 20 K and with ^{129}Xe it is optimal between 100 and 200 K.

The SPINOE is an alternative transfer of spin polarization from laser-polarized gases to surface spins with no requirement for Hartmann-Hahn matching or zero-field mixing. Solidification of the noble gases is not required and consequently the SPINOE can be carried out in a continuous flow mode and over a broader temperature range. Continuous flow would allow signal accumulation and therefore the exploration of surfaces with fewer spins or long relaxation times, as well as SPINOE under magic angle spinning.

ACKNOWLEDGMENTS

The authors are grateful to R. E. Taylor for coating the Aerosil sample with PEO. This work was supported by the Director, Office of Energy Research, Office of Basic Energy Sciences, Materials Sciences Division, of the U.S. Department of Energy under Contract No. DE-AC03-76SF00098. Partial support was also provided by the Office of Naval Research under Order No. N00014-95-F-0099. S.A. was partially supported by the Deutsche Forschungsgemeinschaft; E.L.H and T.R. were partially supported by the National Science Foundation through Grant No. FD93-11913 administered by the Department of Physics. R.S. acknowledges support from the Swiss National Science Foundation. T.R. was supported by the Molecular Design Institute, Office of Naval Research Order No. N00014-95-F-0099.

*Present address: Department of Physics and Astronomy, McMaster University, Hamilton, Ontario L8S 4M1, Canada. Permanent address: Institute of Chemical Physics and Biophysics, Akadeemia tee 23, Tallinn, EE0026, Estonia.

†Present address: Department of Physics, Princeton University, New Jersey 08544.

[1] T. Ito and J. Fraissard, J. Chem. Phys. **76**, (1982); J. Reisse, New J. Chem. **10**, 665 (1986); J. Ripmeester, C. Ratcliffe, and J. Tse, J. Chem. Soc., Faraday Trans. I **84**, 3731 (1988); C. Dybowski, N. Bansal, and T. Duncan, Annu. Rev. Phys. Chem. **42**, 433 (1991); C. Jameson, A. Jameson, R. Gerald, and A. de Dios, J. Chem. Phys. **96**, 1676 (1992); D. Raftery and B. Chmelka, in *NMR Basic Principles and Progress*, edited by B. Blümich and R. Kosfeld (Springer, Heidelberg, 1994), Vol. 30.

[2] G. Cho, L. M. Moran, and J. P. Yesinowski, Appl. Magn. Res. **8**, 549 (1995).

[3] H. Middleton *et al.*, Magn. Res. Med. **33**, 271 (1995).

[4] M. S. Albert *et al.*, Nature **370**, 199 (1994).

[5] M. Leduc and E. Otten, La Recherche **287**, 41 (1996).

[6] T. E. Chupp *et al.*, Phys. Rev. Lett. **63**, 1541 (1989); T. E. Chupp and R. J. Hoare, *ibid.* **64**, 2261 (1990).

[7] S. Appelt, G. Waeckerle, and M. Mehring, Phys. Lett. A **204**, 210 (1995).

[8] D. Raftery *et al.*, Phys. Rev. Lett. **66**, 584 (1991).

[9] H. W. Long *et al.*, J. Am. Chem. Soc. **115**, 8491 (1993).

[10] H. C. Gaede *et al.*, Appl. Magn. Res. **8**, 373 (1995).

[11] T. Pietrass and H. Gaede, Adv. Mater. **7**, 826 (1995).

[12] C. R. Bowers *et al.*, Chem. Phys. Lett. **205**, 168 (1993).

[13] B. Driehuys, G. D. Cates, and W. Happer, Phys. Lett. A **184**, 88 (1993).

[14] B. Driehuys, G. D. Cates, and W. Happer, Phys. Rev. Lett. **74**, 4943 (1995).

[15] A. Bifone *et al.*, Phys. Rev. Lett. **74**, 3277 (1995).

[16] G. Navon *et al.*, Science **271**, 1848 (1996).

[17] A. W. Overhauser, Phys. Rev. **91**, 476 (1953); **92**, 411 (1953).

[18] T. R. Carver and C. P. Slichter, Phys. Rev. **92**, 212 (1953); **102**, 975 (1956).

[19] S. R. Hartmann and E. L. Hahn, Phys. Rev. **128**, 2042 (1962).

[20] L. J. Friedman, P. Millet, and R. C. Richardson, Phys. Rev. Lett. **47**, 1078 (1981).

[21] F. W. V. Keuls, R. W. Singerman, and R. C. Richardson, J. Low Temp. Phys. **96**, 103 (1994).

[22] *Basic Characteristics of AEROSIL*, Vol. 11 of *Technical Bulletin Pigments*, 4th ed. (Degussa, Akron, OH 1993).

[23] The intensity of the total signal (adsorbed plus solid phase) does not follow the T^{-1} Curie law, implying that some of the solid Xe has a very long relaxation time.

[24] A. Abragam, *Principles of Nuclear Magnetism* (Oxford University Press, New York, 1961).

[25] In order to obtain the opposite noble gas nuclear spin magnetizations the direction of the magnetic field in the optical pumping setup is reversed with respect to the propagation direction of the circularly polarized light, without changing the light helicity.

[26] I. Solomon, Phys. Rev. **99**, 559 (1955).

[27] E. Stejskal, J. Schaefer, J. Henis, and M. Tripodi, J. Chem. Phys. **61**, 2351 (1974).

[28] J. H. Noggle and R. E. Schirmer, *The Nuclear Overhauser Effect: Chemical Applications* (Academic Press, New York, 1975).